Removal and Recovery of Silver by Dynamic Adsorption on Bentonite Clay Using a Fixed-Bed Column System

M. L. Cantuaria[1], E. S. Nascimento[1], A. F. Almeida Neto[1], O. A. A. dos Santos[2] and M. G. A. Vieira[1,*] *(1) Department of Process and Products Design, School of Chemical Engineering, University of Campinas (UNICAMP), Avenida Albert Einstein, 500, CEP 13083-852, Campinas, São Paulo, Brazil. (2) Department of Chemical Engineering, University of Maringá, UEM, Avenida Colombo, 5790, CEP 87020-900, Maringá, Paraná, Brazil.*

(Received date: 20 July 2014; Accepted date: 20 December 2014)

ABSTRACT: Several studies have focused on the removal and recovery of precious metal ions from industrial wastewater due to their environmental and economic importance. Adsorption on bentonite clays has been shown to possess a high removal potential for several metal ions. We herein investigated the dynamic adsorption of silver using a fixed-bed column and a calcined bentonite clay called *Verde-lodo* as an adsorbent. A fluid dynamic study was performed to evaluate the adsorption system's metal-ion removal capacity (q_u and q_t), the mass transfer zone and the percentage of total removal according to different effluent's flow. Adsorption–desorption cycles were carried out using nitric acid as an eluent to evaluate the useful lifetime of the column. The breakthrough curves were fitted to the Bohart–Adams model (quasichemical). Moreover, the zeta potential was analyzed to explain the difference between the removal capacity obtained for the static and dynamic systems.

1. INTRODUCTION

Wastewater contaminated with heavy metals has been the subject of much research because of the several problems that it may cause to the environment and human health. The pollution caused by these components increases continuously due to the rise of industrial activity (Fu and Wang 2011). Various methods (e.g. membrane filtration, solvent extraction and others) have been studied to remove and/or recover these metals (Kentish and Stevens 2001). Among these methods, adsorption is being considered a method with many benefits, especially when it comes to its efficiency and low cost (Almeida Neto *et al*. 2012; Vieira *et al*. 2014).

In this method, the choice of the adsorbent is extremely important and the use of low-cost adsorbents is the focus of many studies (Sari and Tüzen 2013). Clays have been demonstrated to have good potential in the removal of metal ions and other pollutants from wastewater because of their important characteristics (e.g. high superficial area and physical and chemical stability; Bailey *et al*. 1999; Chen *et al*. 2008). Therefore, several types of clay minerals such as illite, sepiolites and montmorillonites have been recently investigated (Anirudhan *et al*. 2012).

Among the heavy metals considered as industrial pollutants, silver plays an important role. The main reason for this is its widespread use in industrial activities such as the production of battery, mirrors and photographic film, and also as a disinfectant agent in the pharmaceutical and food industries (Çoruh *et al*. 2010). This metal, in elevated concentrations, may cause several negative

*Author to whom all correspondence should be addressed. E-mail: melissagav@feq.unicamp.br (M.G.A. Vieira).

health effects like argyria (disease that causes skin pigmentation) and liver and kidney degeneration (Fung and Bowen 1996; Song *et al*. 2011). Silver may also be accumulated in human organs such as the brain and muscles (Venugopal and Luckey 1978).

In order to guarantee the effectiveness of an adsorption process with a large-scale application, it is essential to evaluate process parameters in both static and dynamic systems (Nishikawa *et al*. 2012). Although several studies have presented results related to silver's adsorption in the static system (Khan *et al*. 1995; Sari and Tüzen 2013), there is a lack of knowledge regarding the evaluation of silver's adsorption in a dynamic system. In this study, the adsorption of silver using a bentonite clay called *Verde-lodo*, from the state of Paraíba in Brazil, was investigated in a fixed-bed column. This clay demonstrated good affinity towards silver in a previous study (Cantuaria *et al*. 2014b) and was thus chosen for this work. Furthermore, three adsorption–desorption cycles were carried out using nitric acid as eluent to verify the recovery efficiency of the system. Finally, a zeta potential study was performed, which explained the higher removal capacity in the dynamic adsorption system compared with the static adsorption of silver.

2. EXPERIMENTAL

2.1. Reagents and Equipment

Silver solution (concentration of 100 mg/l) was prepared by the dissolution of silver nitrate ($AgNO_3$; Merck, Germany) in deionized water. A nitric acid solution (concentration of 0.1 mol/l) was prepared by diluting a solution of nitric acid (Chemco, Brazil).

Silver concentrations were determined by atomic absorption spectroscopy using a spectrophotometer (AA-7000; Shimadzu, Japan). To guarantee the efficiency of the measure, the samples were diluted using an automatic pipette (Gilson, USA).

2.2. Preparation of the Adsorbent

The adsorbent used in this study is a bentonite clay called Verde-lodo from the Northeast of Brazil and commercialized by the company Dolomil Ltd. The clay was crushed with a grinder and then sieved to the average diameter of 0.855 mm. The clay was then thermally treated (calcination) to increase its resistance and stability, which are important characteristics for its applicability in column systems. This process was carried out in a muffle (QUIMIS, Brazil) at the temperature of 500 °C.

The chemical composition of raw clay obtained by X-ray fluorescence analysis was reported by Almeida Neto *et al*. (2012), and is as follows: 54.29% SiO_2, 19.71% Al_2O_3, 9.27% Fe_2O_3, 3.3% MgO, 1.3% TiO_2, 0.76% CaO, 0.64% Na_2O, 1.94% K_2O, 0.06% P_2O_5 and 8.72% loss on ignition at 1273 K (LOI). The chemical composition published by Almeida Neto *et al*. (2012) for calcined Verde-lodo clay obtained using X-ray fluorescence analysis is 54.13% SiO_2, 19.36% Al_2O_3, 15.14% Fe_2O_3, 4.13% MgO, 0.93% TiO_2, 0.48% CaO, 0.27% Na_2O, 1.08% K_2O, 0.05 P_2O_5 and 4.38% LOI. Based on the quantity of charge-compensating cations reported by Almeida Neto *et al*. (2012), the theoretical cation-exchange capacity calculated were 88 and 48 meq/100 g for raw Verde-lodo and calcined Verde-lodo, respectively. Powder diffraction data of raw Verde-lodo and calcined Verde-lodo samples were collected using a PHILIPS X'PERT X-ray powder diffractometer, equipped with a graphite monochromator and a Cu tube, operating at 40 kV and 40 mA. The analyses were performed with Cu-K_α radiation [step size (2θ), 0.02°].

2.3. Column System Assembly

The experiments were performed in a glass column (internal diameter, 1.5 cm) filled with Verde-lodo clay until a bed height of 15 cm is achieved. The silver solution was passed through the column in an upflow stream using a peristaltic pump (Masterflex, USA). The automatic fraction collector FC203 (Gilson) was used to collect the effluent samples at previously determined time intervals. All experiments were performed at room temperature and the adsorbent was first rinsed with 100 ml of deionized water. The system used for all the assays in this study is shown in Figure 1.

The first experiment was conducted using three different flow rates (3, 4 and 5 ml/minute) to identify the optimum condition for the silver removal in a dynamic system. The parameters evaluated were the adsorption system's metal-ion removal capacity (q_u and q_t), the mass transfer zone (MTZ) and the percentage of total removal.

Using the best flow rate determined by the first experiment, another adsorption cycle was performed to reach the saturation of the bed again followed by a desorption cycle to recover the amount of metal previously adsorbed. To select the eluent compound for this study, the following seven eluents were tested in a static system to verify their desorption capacity: nitric acid (HNO_3), sodium chloride (NaCl), calcium chloride ($CaCl_2$), hydrochloric acid (HCl), thiourea [$SC(NH_2)_2$], sodium phosphate (NaH_3PO_4) and sulphuric acid (H_2SO_4). Of all these eluents, sulphuric and nitric acid yielded the best desorption capacity for silver. This result may be justified by the fact that HNO_3 and H_2SO_4 are classified as strong acids with ionizable hydrogen that could substitute silver adsorbed on the clay. Although H_2SO_4 presented good desorption capacity, it has two ionizable hydrogens that may attack the structure of the clay more strongly than HNO_3 during silver desorption. Therefore, nitric acid was used as eluent for these assays, which is in accordance with other studies where this acid was used (Mattuschka and Straube 1993; Vernon and Zin 1981). After the first desorption cycle, two more adsorption–desorption cycles were carried out to verify whether the adsorbent had maintained its adsorption capacity.

2.4. Column System Analysis

In order to verify the removal of silver during the experiments, some important parameters were calculated. The capacity of silver removal was verified by the amount of total removal up to the

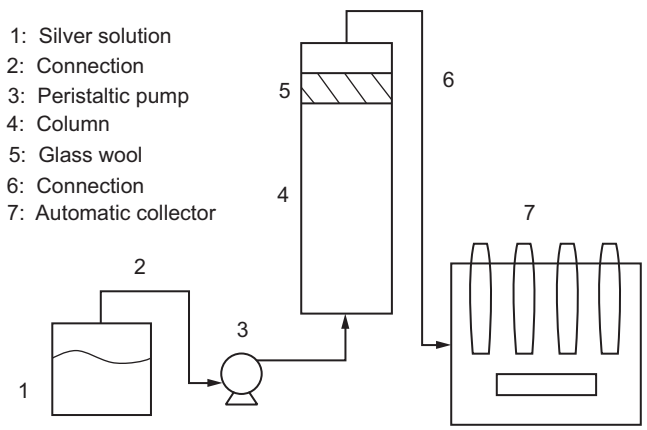

Figure 1. Experimental system used for the column system experiments.

saturation point (q_t) and the amount of useful removal (i.e. up to 5% of the initial concentration in outlet flow) up to the breakthrough point (q_u). These parameters were calculated using equations (1) and (2), obtained by the mass balance in the column.

$$q_t = \frac{C_0 \times Q}{m} \int_0^{\infty} \left(1 - \frac{C}{C_0}\right) dt \tag{1}$$

$$q_u = \frac{C_0 \times Q}{m} \int_0^{t_r} \left(1 - \frac{C}{C_0}\right) dt \tag{2}$$

where C_0 is the initial concentration of silver (mmol/l), Q is the flow used in the system (l/minute), m is the mass of the adsorbent added in the column (g), C is the concentration of silver at time t and t_r is the time up to the rupture point (minutes). The integration part was calculated by the area below the curve $1 - C/C_0$ versus time up to the bed exhaustion (q_t) and up to the breakthrough point (q_u). The area was calculated with *Origin 6.0*.

The MTZ was calculated using equation (3) (Geankoplis 1993)

$$MTZ = \left(1 - \frac{q_u}{q_t}\right) \times H_L \tag{3}$$

where H_L is the bed height. When the amount of useful removal of silver is zero, the maximum value of MTZ is obtained, which is equal to the value of the bed height. Therefore, the ideality is reached when MTZ is zero, which means that the lower the value of MTZ, the better is the removal process efficiency.

Another parameter calculated in this study was the percentage of total removal (%RT). This parameter is calculated by comparing the amount of silver adsorbed from the total metal concentration in the effluent up to the saturation point. The amount of silver adsorbed is verified by the area below the curve $1 - C/C_0$ versus time.

To evaluate the desorption process, the eluted amount of silver was calculated using equation (4) (Voleski *et al*. 2003)

$$q_{el} = \frac{Q}{m} \int C_{el}\, dt \tag{4}$$

where C_{el} is the silver concentration after the elution process at time t. The integration part is calculated by the area below the elution curve (C_{el} vs. time). The percentage of elution (%E) was also calculated considering the amount of total removal (q_t) as 100% of the metal that could be eluted from the adsorbent.

The Bohart–Adams model, also known as *quasichemical*, was used to fit the breakthrough curves of this study. The removal ratio of silver is described by equation (5) (Ruthven 1984)

$$\frac{C}{C_0} = \frac{e^{\tau}}{e^{\tau} + e^{\xi} - 1} \tag{5}$$

The parameters t and ξ are calculated using equations (6) and (7)

$$\tau = kC_0\left(t - \frac{z}{v}\right) \tag{6}$$

$$\xi = \frac{kq_0 z}{v}\left(\frac{1-\varepsilon_L}{\varepsilon_L}\right) \tag{7}$$

where z is the bed height, v is the fluid flow velocity and ε_L is the bed's porosity. The parameter k represents the removal ratio (quasichemical constant) and q_0 represents silver concentration in the adsorbent before the elution process. The adjustments of the curves were made with *Mathcad 2011 Professional*.

2.5. Zeta Potential Measurements

The zeta potential analysis is carried out to evaluate the charge of the particle's surface to verify the electrical charge density for the adsorbent at different pH values. The pH value that provides a surface charge equal to zero is called the *point of zero charge*. The SurPASS Electrokinetic analyzer (Anton Paar, Austria) was used to measure the zeta potential of the adsorbent arranged in a fixed bed, to verify the total charge of the particles when they assume the disposition of dynamic system adsorption process. This result was compared with the zeta potential measurement obtained by potentiometric titration that represents the adsorption in the static system (Almeida Neto *et al*. 2012).

The calcined Verde-lodo clay was first rinsed for 18 hours by constant stirring to eliminate small particles. Approximately 0.2 g of the clay was added to the cylinder cell and later compacted. For this technique, a solution of ammonium acetate (0.1 mol/l; CH_3COONH_4) was used as an electrolyte and acetic acid (6 mol/l; CH_3COOH) and ammonium hydroxide (0.25 mol/l; NH_4OH) were used as acid and base, respectively.

3. RESULTS AND DISCUSSION

X-ray powder diffraction patterns for natural and calcined Verde-lodo clay are shown in Figure 2. The result is typical of smectites with a broad 001 reflection. The characteristic montmorillonite peak is reduced in the calcined Verde-lodo sample when compared with the raw clay sample, which is expected for materials subjected to thermal treatments. Although the raw Verde-lodo sample reached a peak in the region of 0.723 nm, which relates to kaolinitic clay, the same peak was not detected after calcination. In both clays, the presence of other peaks in the following ranges can be observed: 0.45 and 0.41 nm corresponding to smectite; 0.32 and 0.25 nm corresponding to quartz and 0.15 nm corresponding to the broad 060 reflection, suggesting that they are bi-octahedral smectite (Brindley and Brown 1980).

3.1. Study of Different Flow Rates

Dynamic experiments were carried out for different flow rates: 3, 4 and 5 ml/minute. The breakthrough curves are shown in Figure 3. Overall, as seen from Figure 3, the curves presented a behaviour close to the ideal, which is characterized by an abrupt step change in the rupture

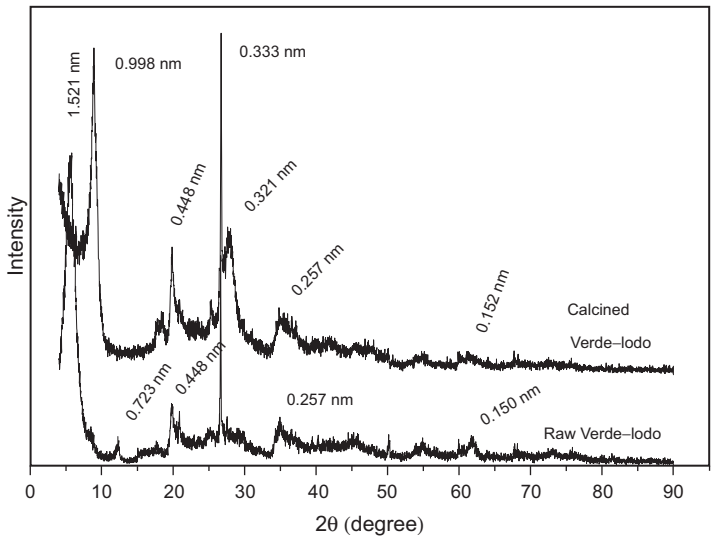

Figure 2. X-ray diffractograms of raw Verde-lodo and calcined Verde-lodo.

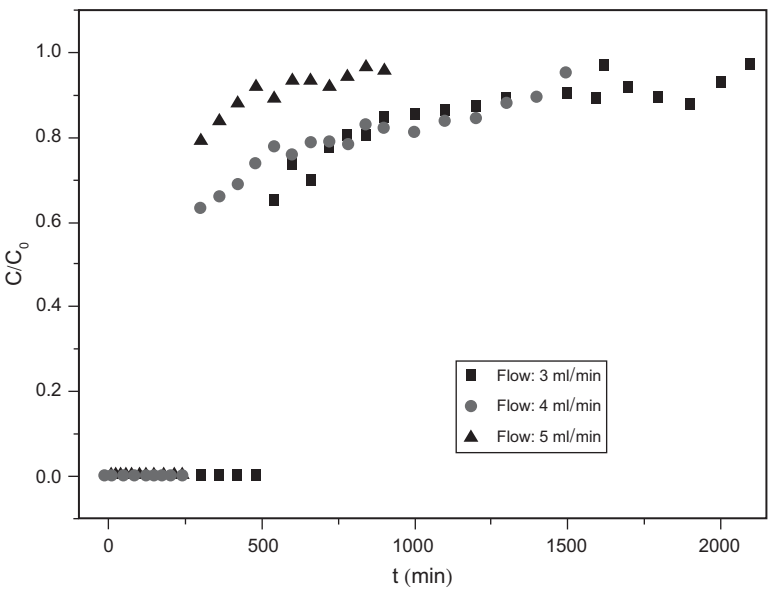

Figure 3. Breakthrough curves obtained for the three flow rates analyzed: 3, 4 and 5 ml/minute.

point's region. In addition, they presented a resistance to bed saturation. The parameters obtained for the experimental curves are presented in Table 1.

The optimum flow rate was selected according to the parameters presented in Table 1. Although the flow of 3 ml/minute presented higher values for the amount of total and useful removal (q_t and q_u), the choice was made based on the percentage of total removal (%RT) and the MTZ. The adsorption process is more efficient when the percentage of total removal is higher and the MTZ is lower. When comparing the values, the flow rate 5 ml/minute showed

better results, and thus was selected for the next assays. The breakthrough curves shown in Figure 3 were fitted by the Bohart–Adams model. Figure 4 shows the *quasichemical* adjustment for the experiment with the flow rate of 5 ml/minute. The other flow rates presented a similar fitting curve. Table 2 presents the parameters k and q_0 obtained for the three flows analyzed.

The parameters presented in Table 2 demonstrate that the *quasichemical* constant k increases with the increase in the flow rate used in the assay. This fact reveals that a high flow rate increases the removal rate of the silver. The parameter q_0 represents the concentration of silver in the adsorbent, indicating that this concentration was higher for the 3 ml/minute flow.

TABLE 1. Parameters Obtained for the Experimental Breakthrough Curves

	Flow rate (ml/minute)		
Parameters	3	4	5
q_t (mmol/g)	0.250	0.230	0.191
q_u (mmol/g)	0.164	0.063	0.139
MTZ (cm)	5.182	10.887	4.085
%RT	32.62	34.00	36.61

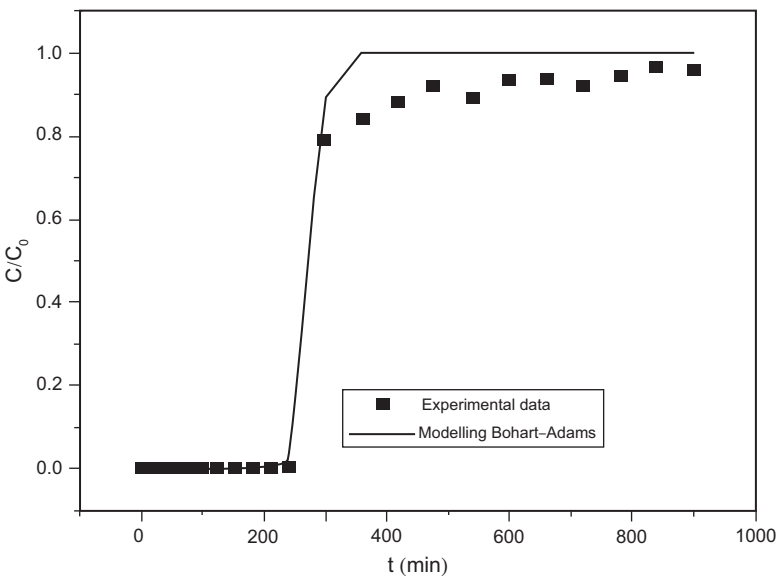

Figure 4. Bohart–Adams adjustment for the breakthrough curve of silver removal using a flow rate of 5 ml/minute.

TABLE 2. Bohart–Adams Parameters Obtained for the Three Analyzed Flows

	Flow rate (ml/minute)		
Parameters	3	4	5
k (l/mmol/minute)	0.0018	0.020	0.036
q_0 (mmol/g)	300	240	290

The solvent recovery efficiency (SRE) describes the relationship between the volume of water used to prepare the eluents (V_E) and the volume of purified water until the breakthrough point (V_b) was achieved. These values are presented in Table 3 for the three flow rates. According to Table 3, the flow rate of 4 ml/minute presented the lower SRE, which is not a favourable result. Although the result is slightly better for 3 ml/minute, the flow 5 ml/minute was still selected for the next assay.

3.2. Adsorption and Desorption Cycles

The previous assays showed that 5 ml/minute was considered to be the best flow to perform the dynamic adsorption of silver using Verde-lodo clay. Thus, three adsorption–desorption cycles were carried out to verify the breakthrough curves after the regeneration of the adsorbent. Figure 5 shows the adsorption curves obtained for the three different cycles and Table 4 presents the parameters calculated for the experimental data.

Figure 5 shows that the first removal cycle showed the same behaviour (close to the ideal), with an abrupt step change in the rupture point's region, which was expected. However, the following removal cycles moved away from the original behaviour, presenting a more extensive region between the rupture point and the exhausting point. This fact indicates that the regeneration

TABLE 3. Solvent Recovery Efficiency of the Adsorption Process

	Flow rate (ml/minute)		
Parameters	3	4	5
V_E (ml)	4960	6000	4500
V_b (ml)	1440	960	1200
SRE (%)	29.0	16.0	26.7

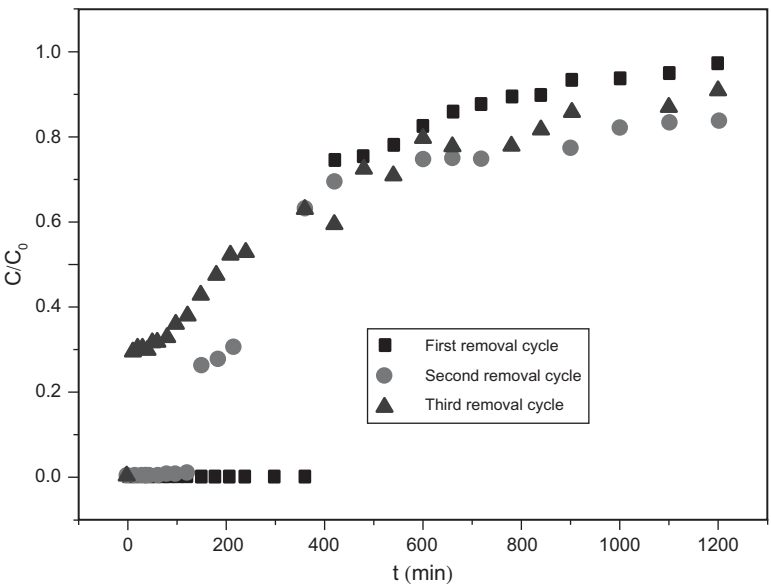

Figure 5. Breakthrough curves obtained for the three adsorption cycles.

process changes the characteristics of the fixed-bed adsorption. Besides that, during the last removal cycle, the flow rate decreased to approximately half of its original value. This occurrence indicates that the dynamic adsorption of silver by Verde-lodo clay should be carried out in two removal/regeneration cycles, at the most.

The results shown in Table 4 for the first and second cycles demonstrated a reduction of the removal efficiency, which was expected. This fact may be observed by the decrease in the amount of total removal (q_t), the amount of useful removal (q_u) and the percentage of removal (%RT). The MTZ values have also increased significantly, showing that the process is moving away from the ideal.

As mentioned earlier, the third cycle presented a change in the flow rate due to the exhaustion of the column. However, even in the third cycle, the bed maintained its adsorption capacity after the regeneration process using HNO_3 as the eluent. Furthermore, the amount of the useful removal until the breakthrough point (q_u) was zero. This means that the silver was not completely adsorbed even at the beginning of the experiment (Figure 5). As a result, the value of MTZ was 15 cm, which is the maximum. This result indicates that the behaviour found was the furthest from the ideal.

The curves of the three adsorption cycles were fitted by the Bohart–Adams model. Table 5 presents the parameters obtained for the first and second cycles. Because of the behaviour of the third cycle, this breakthrough curve could not be adjusted using the quasichemical model. The comparison of the Bohart–Adams parameters for the first and second adsorption cycles reveals that the constant k decreases with the cycle's sequence and that the regeneration of the column modifies the removal ratio of silver. In addition, the parameter q_0 decreases, implying that the amount of silver adsorbed in Verde-lodo clay is significantly lower in the second cycle. The SRE was also calculated for the first two adsorption cycles (Table 6). This parameter was not verified for the third cycle.

TABLE 4. Parameters Obtained for the Removal Cycles Analyzed

	Removal cycle		
Parameters	First	Second	Third
q_t (mmol/g)	0.178	0.102	0.104
q_u (mmol/g)	0.131	0.026	0
MTZ (cm)	3.96	11.15	15.00
%RT	40.69	38.72	31.01

TABLE 5. Bohart–Adams Parameters Obtained for the First and Second Adsorption Cycles

	Removal cycle		
Parameters	First	Second	Third
k (l/mmol/minute)	0.03	0.018	–
q_0 (mmol/g)	262	110	–

TABLE 6. Solvent Recovery Efficiency for the Removal Cycles

	Removal cycle		
Parameters	First	Second	Third
V_E (ml)	6000	6000	–
V_b (ml)	1800	600	–
SRE (%)	30.0	10.0	–

The SRE is reduced after the regeneration of the column from 30% of recovery to 10% of recovery (Table 6). The results show that this process decreases the column efficiency, which was expected. The silver desorption was verified after the three removal cycles and HNO_3 was used as the eluent. The desorption curves for all the cycles are shown in Figure 6.

Figure 6 demonstrated the typical behaviour of a desorption curve. During the initial time intervals, the concentration of silver was high, indicating an elevated desorption at the beginning of the process. After a while, the silver concentration remains constant showing the limit of the desorption. Both curves present exponential decay behaviour. The curves in Figure 6 show that the final concentration of silver in the first cycle is lower than the final concentration for the second and third cycles. Another way to compare the performance of desorption cycles is by analyzing the eluted amount of silver (q_{el}) and the percentage of elution (%E). These parameters are presented in Table 7.

The results presented in Table 7 reveal that the eluted amount of silver is higher for the first desorption cycle. This fact indicates that the desorption capacity decreases in the sequencing assays. However, the percentage of elution increased according to the cycle number. This fact may be explained by the significantly lower amount of total removal (q_t) during the second and third adsorption cycles. As the percentage of elution is calculated by the comparison between the amount of silver in the column and the eluted amount, this value increased for the last two cycles.

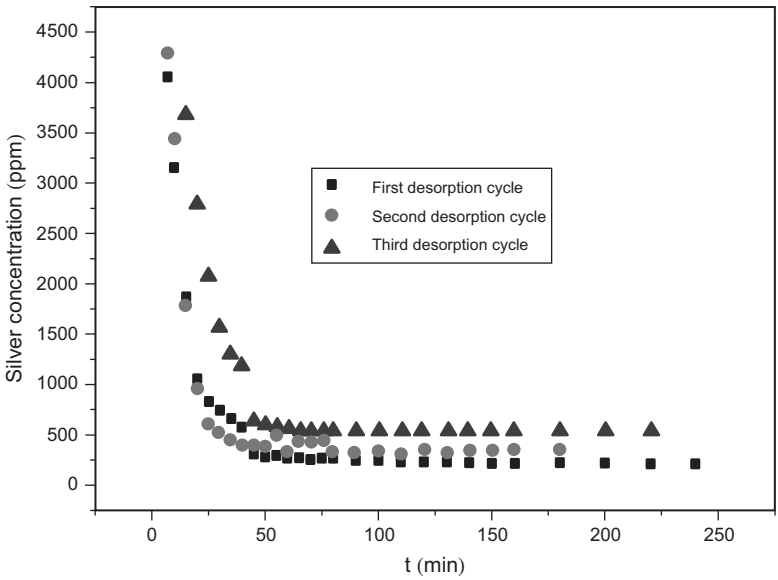

Figure 6. Desorption curves obtained for the adsorbent's regeneration using nitric acid as eluent.

TABLE 7. Parameters Obtained for the Desorption Cycles

	Desorption cycle		
Parameters	First	Second	Third
q_{el} (mmol/g)	0.084	0.067	0.071
%E	47.28	65.63	68.50

3.3. Potential Zeta Analysis

The particle's zeta potential was measured in two different dispositions. Figure 7 shows the potential zeta curve representing the batch system and Figure 8 presents the curve for a dynamic system disposition. From Figure 7, it is possible to verify that, according to the pH, the particles disposed in the static system have negative and positive values for zeta potential and also, in this case, the value for point of zero charge is equal to 5.3. The acid conditions provide higher values of zeta potential due to the addition of H^+ ions. By contrast, the opposite is noted for alkaline conditions.

However, Figure 8 shows that the zeta potential values are entirely negative for the dynamic system disposition. This fact may be explained by the double-layer effect, a model used to explain the effect of the ionic strength in the vicinity of a solid matter. This model states that the electric potential of a particle's surface causes the attraction of ions with an opposite charge, forming an attached layer around the solid matter. This layer, called the *Stern layer*, causes a reduction of the electric potential due the neutralization of the initial charge. Consequently, this reduced potential also attracts ions with an opposite charge, but with a lower intensity (Oliveira *et al*. 2000).

Therefore, to guarantee the double-layer effect, it is necessary to have a distance between the particles. This fact occurs when the particles are in a batch disposition. By contrast, for a fixed-bed system, the particles are compacted and the distance between each other is almost non-existent, which indicates that the double-layer effect does not affect the surface's charge. This fact explains the negative values measured in this arrangement. The difference between the zeta potential values may explain the significant variation obtained for the silver removal capacity for both dispositions. For a static system, the silver removal capacity was shown to be 0.062 mmol/g (Cantuaria *et al*. 2014a), whereas for a dynamic system, the silver removal capacity was 0.25 mmol/g for the flow rate of 3 ml/minute. The difference between these results may be explained by a higher negative charge of the adsorbent, providing a higher attraction of Ag^+ in this system.

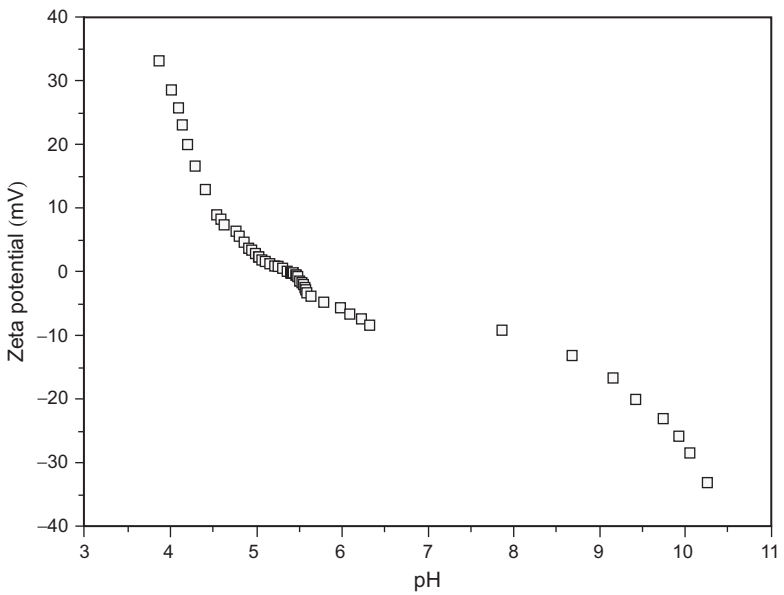

Figure 7. Zeta potential obtained by potentiometric titration representing a static system disposition (adapted from Almeida Neto *et al*. 2012).

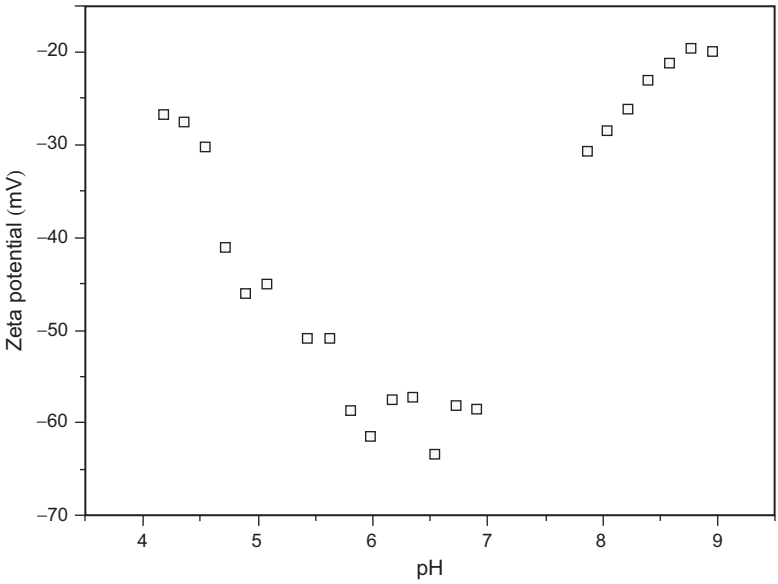

Figure 8. Zeta potential representing a dynamic system disposition.

4. CONCLUSIONS

This study presented several experiments to analyze the dynamic adsorption of silver using a bed column system and calcined bentonite clay called Verde-lodo. The fixed-bed column disposition presents a higher removal capacity when compared with a static adsorption of silver, which is explained by the variation of zeta potential. Results have shown that the breakthrough curves yield a behaviour close to the ideal for the first removal cycle for all the flow rates studied. When comparing the parameters obtained for the different flow rates, the 5 ml/minute flow came up with better results for the MTZ and the percentage of removal.

The following removal cycles were carried out with the selected flow rate. For each removal cycle, the adsorbent was regenerated with nitric acid as the eluent. The following removal cycles moved away from the original behaviour, showing that the desorption process modifies the characteristics of the fixed-bed adsorption. The experimental desorption curves presented an exponential decay behaviour. In addition, all breakthrough curves, with the exception of the third adsorption cycle's curve, were well adjusted by the Bohart–Adams model. The flow rate reduction during the third cycle revealed that dynamic adsorption of silver using Verde-lodo clay should be performed in two adsorption–desorption cycles, at the most.

ACKNOWLEDGEMENTS

The authors thank CNPq, CAPES and FAPESP (Proc. 2013/00732-1) for the financial support.

REFERENCES

Almeida Neto, A.F., Vieira, M.G.A. and Silva, M.G.C. (2012) *Mater. Res*. **15**, 114.
Anirudhan, T.S., Bringle, C.D. and Radhakrishnan, P.G. (2012) *Chem*. *Eng*. *J*. **200–202**, 149.
Bailey, S.E., Olin, T.J., Bricka, M. and Adrian, D. (1999) *Water Res*. **33**, 2469.
Brindley, G.W. and Brown, G.E. (1980) *Crystal Structures of Clays Minerals and Their X-Ray Identification*, Mineralogical Society, London, UK.
Cantuaria, M.L., Almeida Neto, A.F., Nascimento, E.S., Santos, O.A.A. and Vieira, M.G.A. (2014a) *Chem*. *Eng*. *Trans*. **39**, 667.
Cantuaria, M.L., Almeida Neto, A.F. and Vieira, M.G.A. (2014b) *Chem*. *Eng*. *Trans*. **38**, 109.
Chen, W.J., Hsiao, L.C. and Chen, K.K.Y. (2008) *Process Biochem*. **43**, 488.
Çoruh, S., Senel, G. and Ergun, O.N. (2010) *J*. *Hazard*. *Mater*. **180**, 486.
Fu, F. and Wang, Q. (2011) *J*. *Environ*. *Manage*. **92**, 407.
Fung, M.C. and Bowen, D.L. (1996) *Clin*. *Toxicol*. **34**, 119.
Geankoplis, C.J. (1993) *Transport Processes and Unit Operations*, Prentice-Hall International, Englewood Cliffs, NJ.
Kentish, S.E. and Stevens, G.W. (2001) *Chem*. *Eng*. *J*. **84,** 149.
Khan, S.A., Rehman, R. and Khan, M.A. (1995) *Waste Manage*. **15**, 271.
Mattuschka, B. and Straube, G. (1993) *J*. *Chem*. *Technol*. *Biotechnol*. **58**, 57.
Nishikawa, E., Almeida Neto, A.F. and Vieira, M.G.A. (2012) *Adsorpt*. *Sci*. *Technol*. **30**, 759.
Oliveira, I.R., Studart, A.R., Pileggi, R.G. and Pandolfelli, V.C. (2000) *Dispersão e Empacotamento de Partículas: Princípios e Aplicações em Processamento Cerâmico*, Fazendo Arte, São Paulo, Brazil (in Portuguese).
Ruthven, D.M. (1984) *Principles of Adsorption and Adsorption Processes*, John Wiley & Sons, New York.
Sari, A. and Tüzen, M. (2013) *Microporous Mesoporous Mater.* **170**, 155.
Song, X., Gunawan, P., Jiang, R., Leong, S.S.J., Wang, K. and Xu, R. (2011) *J*. *Hazard*. *Mater.* **194**, 162.
Venugopal, B. and Luckey, T.D. (1978) *Metal Toxicity in Mammals,* Plenum Press, New York.
Vernon, F. and Zin, W.M. (1981) *Anal*. *Chim*. *Acta*. **123**, 309.
Vieira, M.G.A., Almeida Neto, A.F., Silva, M.G.C., Carneiro, C.N. and Melo Filho, A.A. (2014) *Braz*. *J*. *Chem*. *Eng*. **31**, 519.
Voleski, B., Weber, J. and Park, J.M. (2003) *Water Res*. **37**, 297.